

Contract No. 951263

Report No. TE4055-145-68

Thermo Electron Corporation, 85 First Avenue, Waltham, Massachusetts 02154

NINTH QUARTERLY REPORT

SOLAR THERMIONIC

GENERATOR DEVELOPMENT

April 1968

Prepared for

Jet Propulsion Laboratory
Pasadena, California

This work was performed for the Jet Propulsion Laboratory, California Institute of Technology, sponsored by the National Aeronautics and Space Administration under Contract NAS7-100.

This report contains information prepared by Thermo Electron Corporation under JPL subcontract. Its content is not necessarily endorsed by the Jet Propulsion Laboratory, California Institute of Technology, or the National Aeronautics and Space Administration.



NINTH QUARTERLY REPORT

SOLAR THERMIONIC GENERATOR DEVELOPMENT

Summary

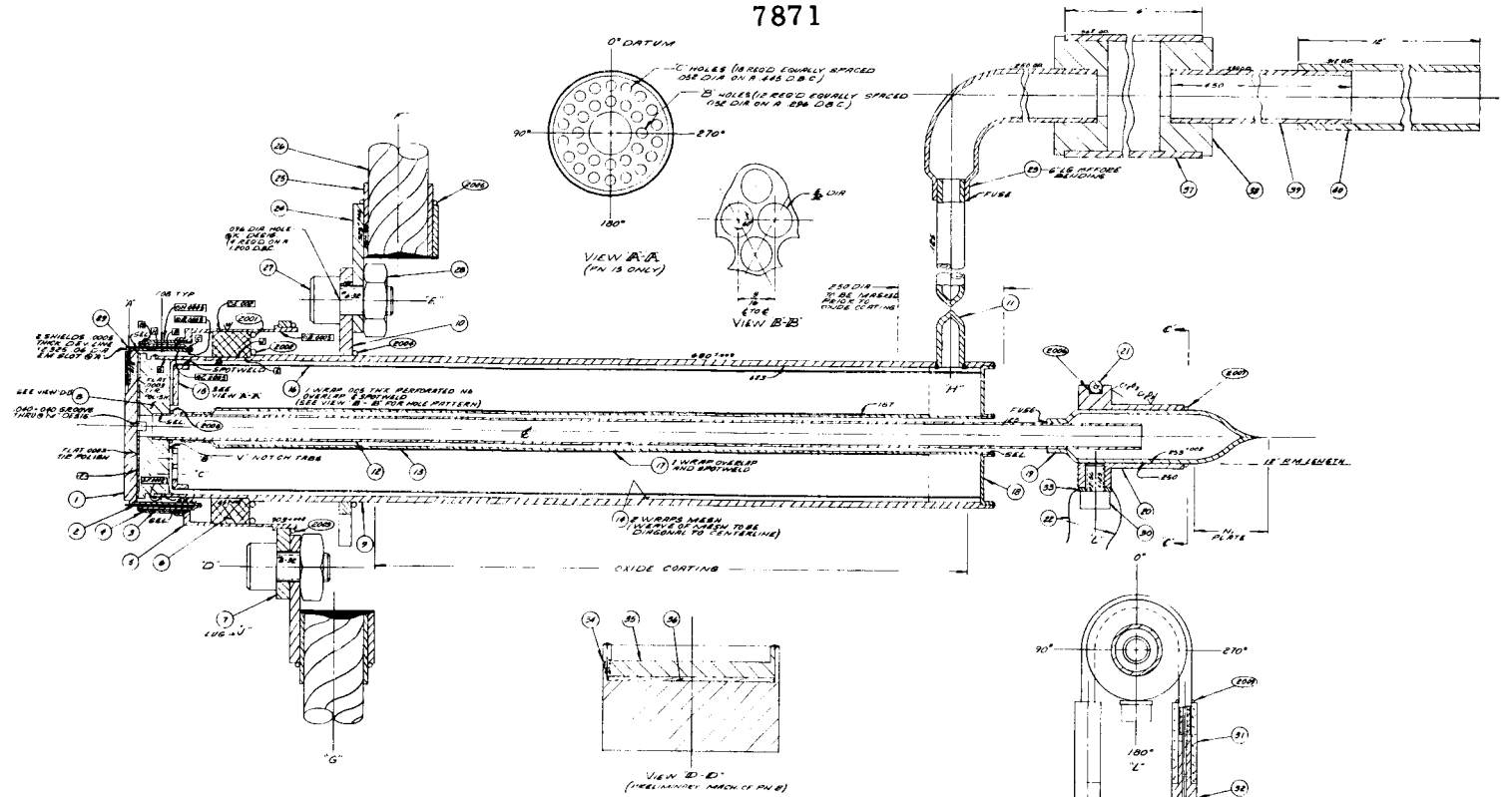
This report covers progress for the ninth quarter, corresponding to the period 1 December 1967 to 29 February 1968.

During this quarter, the fabrication and test of converter T-208 have been completed. This model is the first under this program to incorporate a collector-radiator heat pipe structure. The dynamic performance of converter T-208 was almost identical to that of model T-207 in spite of a 17% reduction in collector area, but the failure of the static data to reproduce the performance data obtained dynamically has shown that the collector of converter T-208 operates at an excessive temperature. The cause of the high collector temperature is believed to be the limited area for vapor flow available at one component of the heat pipe, and it will be corrected in the construction of the following model. In addition, the performance of converter T-208 was relatively low, and cesium conduction tests revealed an unusually large spacing of about 4.4 mils; steps will be taken to improve the positioning of parts during assembly of T-209.

Fabrication of Converter T-208

At the beginning of this quarter, converter T-208 was ready for the assembly of the cesium reservoir tubulation. This is the final assembly operation prior to converter outgassing and cesium charging. In the existing design, shown in Figure 1, the reservoir tubulation, part No. 19, is fuse-brazed to the tantalum tube, part No. 12. To facilitate wetting by the molten copper, and to strengthen the

7871



REV	DESCRIPTION	DATE	BY	APP
1	SEE APP. CO. (P. 24-27)	3-25-67	114	

PART	SIZE	REV	REQ	MATL	NOTES
PICTURES					
21/8					MANU DRILL FORM IN 17
27/8					MANU DRILL FORM IN 18
21/2					1/2" DIA. WIRE FORM IN 11
21/4					1/4" DIA. WIRE FORM IN 11
1/8" B		1	MR		1/8" DIA. B DR 2
1/64" B		1	MR		1/64" DIA. B DR
					</



metallurgical bond between the copper and the tantalum, the tantalum tube is given a very thin nickel electroplate prior to fuse-brazing. In the first two attempts at fuse-brazing the tubulation on converter T-208, a leak-tight bond could not be obtained; consequently, the fuse-brazed tubulation was removed, and the tantalum tube was given a new and thicker nickel electroplate. When a new reservoir tubulation was slipped over the tantalum tube for another fuse-braze attempt, the tantalum tube broke. It was found that the tube had embrittled, apparently during the second fuse-braze, when a high temperature was used, and when the nickel electroplate alloyed with the tantalum. The embrittlement was severe, and it extended along the length of the tantalum tube all the way to the inner weld bead of the end cap of the heat pipe, part No. 18.

The tube could not be replaced without completely dismantling the converter; therefore, a repair was attempted, which consisted of brazing an extension piece to the broken end of the tantalum tube. The extension piece was made of tantalum, and brazed with palladium using an inert-gas arc as the heat source; it has a length of $3/4$ in. , $3/16$ in. of which was machined to slide into the broken end of the converter tube, and it has an inside diameter of 0.065 in.

An attempt to repeat the fuse-braze on this extension failed, and it was concluded that the difficulty in making a successful fuse-braze is caused by the large difference in the diameters of the two tubes being joined; to avoid this difficulty, it was decided to use an intermediate tubular insert, made of niobium, with a diameter of $3/16$ in. This insert was made and joined to the tantalum tube in the exact same manner as the inner heat-pipe tube, part No. 13, and its length was $7/8$ in.



This intermediate piece was welded in place, and the first fuse-braze attempt failed, in part because the niobium tube had not been plated, and in part because the wall thickness of the fuse and of the copper tube was not small enough. A new fuse-braze attempt was made, and it was successful. Upon leak-checking the assembly, however, it was found that the area of the tantalum cesium tube, which had been repaired by means of a palladium braze, had developed a leak. It was subsequently determined that during heliarc-welding of the niobium intermediate tube to the end of the tantalum cesium tube, the area of the tantalum tube which was palladium-brazed overheated to the extent that an alloying reaction between palladium and tantalum occurred and formed a brittle intermetallic. During handling of the assembly to effect the fuse-braze this embrittled area developed a crack and leaked.

The failed assembly just described, which for convenience will be designated as T-208A, could still be repaired by using the internal heat pipe tube, part No. 13 in Figure 1, as the tube to transport the cesium vapor from the cesium reservoir. To accomplish this, the length of the normal cesium tube which protruded beyond the end of the heat pipe was cut off, and a niobium extension piece was copper-brazed to the end of the internal heat pipe tube, part No. 13. A leak-tight assembly was obtained, and a copper tube was fuse-brazed to the niobium extension to serve as the cesium reservoir and outgassing tubulation. Model T-208A was then set up for outgassing, and at the end of a few hours it was evident that sodium was leaking from the heat pipe. Upon examination, it was found that the end cap, part No. 18, had developed a crack midway between the inner and outer welds. At this point further attempts to salvage the assembly 208A were abandoned



because no technique was available for discharging the sodium from a leaking heat pipe, which is a prerequisite to any repair attempt on heat pipe envelopes.

The fabrication of model T-208B proceeded without incident up to the point of cesium reservoir assembly. This reservoir was being constructed by welding an intermediate niobium piece to the end of the tantalum cesium tube, part No. 12, to facilitate fuse-brazing of the copper tubulation, part No. 19. Unfortunately, due to operator error, air was admitted into the welding chamber before the weld was performed, and the joint was completely brittle. The brittle portion of this weld area was removed by cutting the tantalum tube, and an extension piece of tantalum was palladium-brazed to the tantalum tube to continue construction of model 208B. The model was then finally brazed to an emitter structure and prepared for outgassing prior to sodium charging. It was then found that the outer weld of the end cap, part No. 18, was cracked and leaked. Attempts to seal this area by re-welding were not successful, and it was decided to remove the end cap, part No. 18, by machining. Upon removal of the end cap, it was found that the capillary structure was oxidized, and the pattern of this oxidation suggested strongly that it had been caused by a seepage of the nickel electroplating solution which was used to plate the sodium fill tube prior to fuse-brazing it to the heat pipe outgassing and sodium charging tubulation.

The assembly of a third model, designated T-208C, ran into complications during the electron-beam weld of the collector to the heat pipe radiator. To provide better positioning of the collector face with respect to the heat pipe radiator tube, part No. 9, during



electron-beam welding of these two parts, a stainless steel tie rod was inserted through the center of the tantalum cesium tube, part No. 12. The heat developed during electron-beam welding was sufficient to cause melting of the tie rod, however, and the molten metal alloyed with the collector, causing irreparable damage.

The assembly of the fourth model, designated T-208D, was successful. It was accomplished with a new set of parts, and in accordance with the layout of Figure 1, with the following exceptions: The cesium tube, part No. 12, was made of niobium, with an 0.025-in. wall thickness, to avoid using the relatively fragile 0.010-in. wall tantalum tube used in the previous heat pipe converter models. As in previous models, the central capillary, part No. 17 was omitted. A thicker end cap, part No. 18, was used to avoid crack leaks due to possible exposure to embrittling atmospheres or processes. An extension of 3/16-in. -dia niobium tubing was used to connect the cesium tube, part No. 12, to the cesium reservoir tube, part No. 19, as described in the assembly of model T-208A, and for the purpose of reducing the dissimilarity in tube diameters that would occur at the joint of parts Nos. 12 and 19. The rhenium collector face was vanadium-brazed to the niobium substrate because of the unavailability of the AEC pressure-bonding facility which would otherwise have been used. Nickel plating of the ends of both tubes, Nos. 12 and 11, was performed using a pair of small rubber plugs to avoid seepage of plating solution inside the tubes. A 3/16-in. -dia niobium tubing extension was used to connect the sodium fill tube, part No. 11, to the sodium reservoir discharge tube, part No. 23. Also, to avoid joining tubes which differ excessively in diameter, this extension was first fuse-brazed to the sodium discharge tube, and then it was



electron-bombardment brazed to the sodium fill tube using two rings of nickel-plated 0.020-in. -dia copper.

The electroetched emitter was thermally stabilized at approximately 2050°C for 2 hours, at a vacuum of 10^{-5} torr. The maximum deviation from flatness measured after thermal stabilization was 0.004 in.

The assembled model was then connected to a vacuum station to outgas the heat pipe portion of the envelope. The heat pipe was maintained at an average temperature of 490°C with resistance heaters for a period of 16 hours. At the end of this time the sodium ampoule was broken by crushing the walls of the copper manifold where it was located, the argon of the ampoule was pumped out, and the assembly was pinched off. It was then placed in an oven at 150°C for 2 hours to melt the sodium, and the sodium was then transferred into the heat pipe. Following this operation the sodium manifold was pinched off, and the niobium fill tube was cut and sealed with an electron beam.

The next assembly operation consisted of connecting the cesium reservoir with a fuse-braze. That assembly was then connected to the same vacuum station to outgas the converter envelope and proceed with cesium charging. During outgassing of the converter envelope, a radiation shield was wrapped around the heat pipe radiator to help maintain high collector temperatures. The heat pipe was at 800°C, and the radiator temperature was uniform. Converter outgassing was performed for a period of 26 hours with the emitter at an observed temperature of 1700°C. The cesium was then distilled at 200°C for 4 hours.



Test of Converter T-208

The test of converter T-208 consisted of 7 runs as follows: Runs 1 to 3 to map the output under dynamic conditions at 2000, 1900 and 1800°K, Run 4 to measure interelectrode spacing via cesium conduction, and Runs 5 to 7 to map the output under static conditions at 1700, 1600 and 1800°C. The Appendix presents the data collected during test.

During these tests it was found that the cesium reservoir tends to run hotter than in previous heat pipe models owing to the heavier 0.025-in. wall of the cesium tube. Since the previous models (T/E-3 and T/E-4 developed under JPL Contract 951465) have shown that there is no problem in achieving lower reservoir temperatures with an 0.010-in. -wall tube, it is clear that the cesium reservoir temperature can be lowered later with little difficulty. Corrective steps would be difficult to implement within the remaining period of contract performance due to the long lead time required to procure small-diameter niobium tubing, but solution can be postponed because the cesium reservoir temperature is still low enough to permit optimization at all operating conditions of interest.

Figure 2 presents a summary of the optimized I-V characteristics; the solid lines are the characteristics obtained by dynamic test, and the dashed ones were obtained statically.

Figure 3 presents the cesium conduction data.

Interpretation of Converter T-208 Test Results

Converter T-208 used rhenium electrodes, and it is therefore of interest to compare its performance with that of converter T-206, which also used rhenium electrodes. It will be recalled that converter T-207, fabricated in the interim, had a palladium collector.

8267

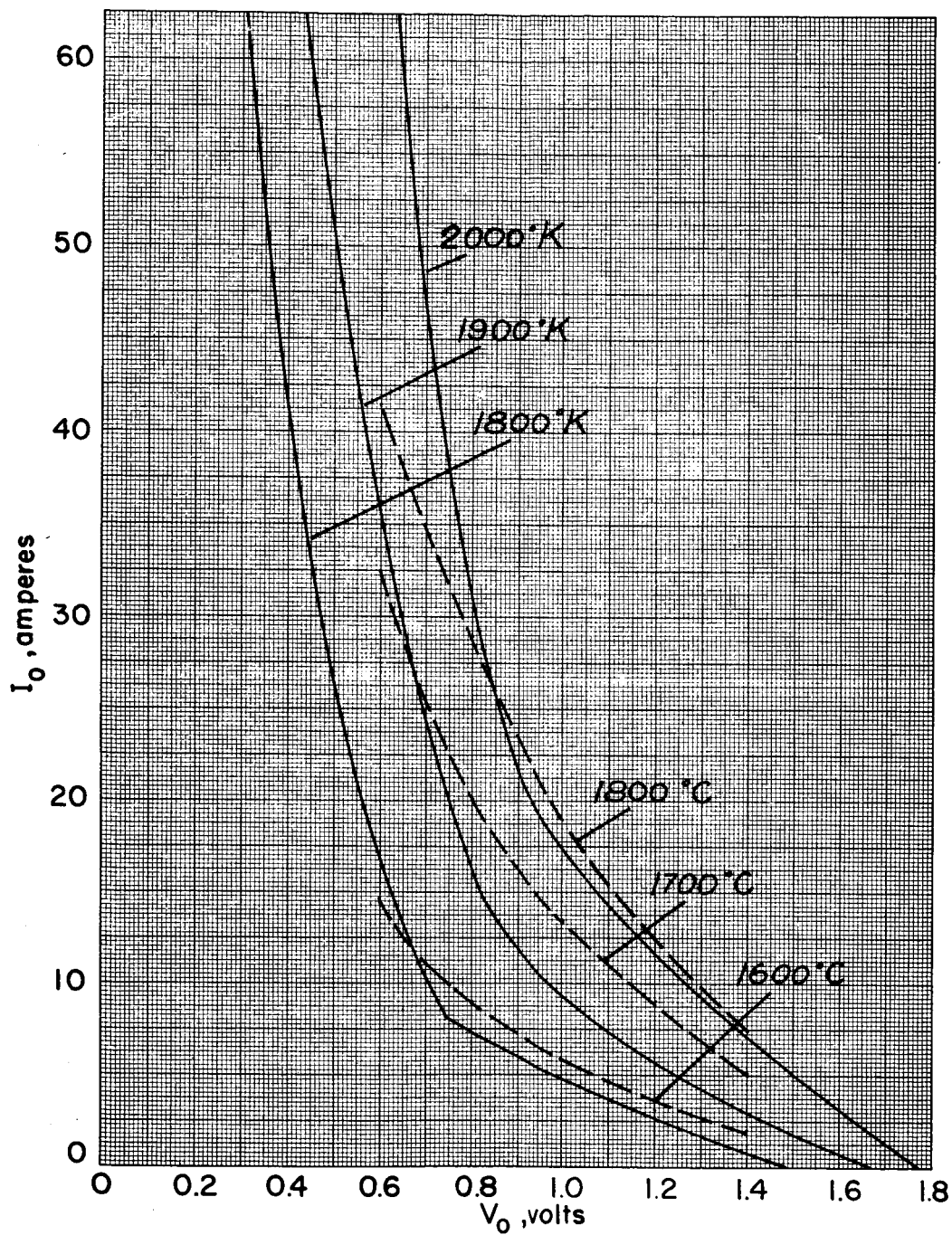


Figure 2



8268

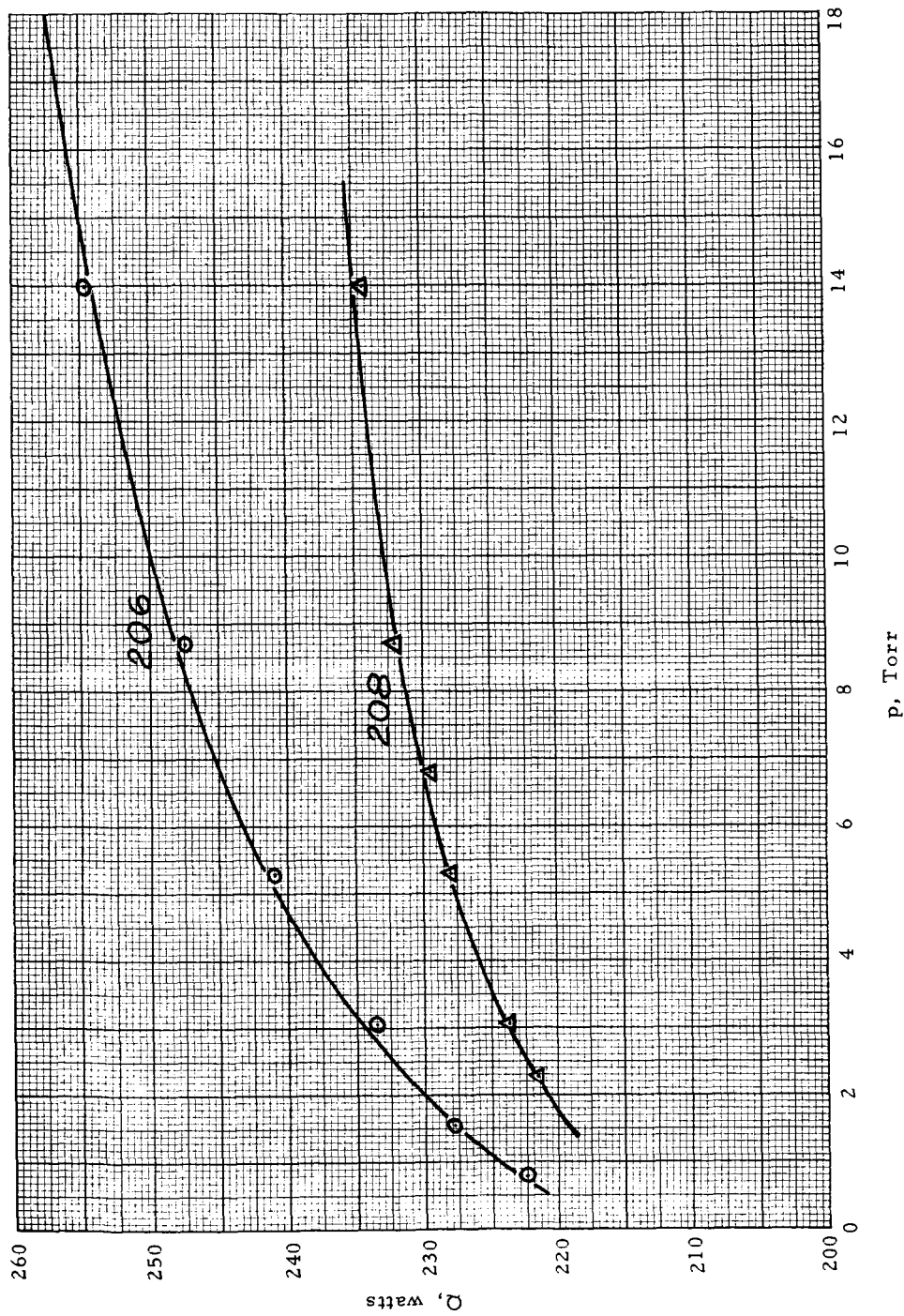


Figure 3



Before a performance comparison of the two converters is made, it is well to review their differences in structure. Converter T-206 had a finned radiator and was assembled using well developed procedures; in addition, it had a collector diameter of 0.705 in., corresponding to a collector electrode area of 2.52 cm^2 . Converter T-208 used a heat pipe radiator structure for the first time in this program, which was assembled according to untried procedures; furthermore, its collector diameter had to be decreased to 0.680 in. because of reduced tolerance control in the heat pipe structure assembly. This diameter corresponds to an area of 2.34 cm^2 , which is further reduced by the slot used for outgassing purposes, shown in Figure 1, and the reduction is 0.18 cm^2 , leaving a net electrode area of 2.16 cm^2 . The effective electrode area of converter T-208 was then $2.16/2.52 = 0.86$ times the electrode area of converter T-206.

Figures 4, 5 and 6 give the comparison of the dynamic characteristics of converters T-206 and T-208, at emitter temperatures of 1800, 1900, and 2000°K, respectively. In order to subtract the effect of the 14% reduction in collector area of converter T-208, the figures show, in dashed lines, the effect of reducing the output current values of converter T-206 by 14%. As can be seen, converter T-206 is able to produce a consistently higher output voltage. In the ignited mode, the increment in output voltage increases with emitter temperature; thus at 1800°K it is approximately 60 mV, at 1900°K it is approximately 120 mV, and at 2000°K it is approximately 160 mV. A detailed examination of the individual I-V curves obtained for the determination of the envelopes shown in these figures shows that, for the same output current density and emitter temperature, the optimum cesium pressure was the same in the two converters, and that the optimum

8269

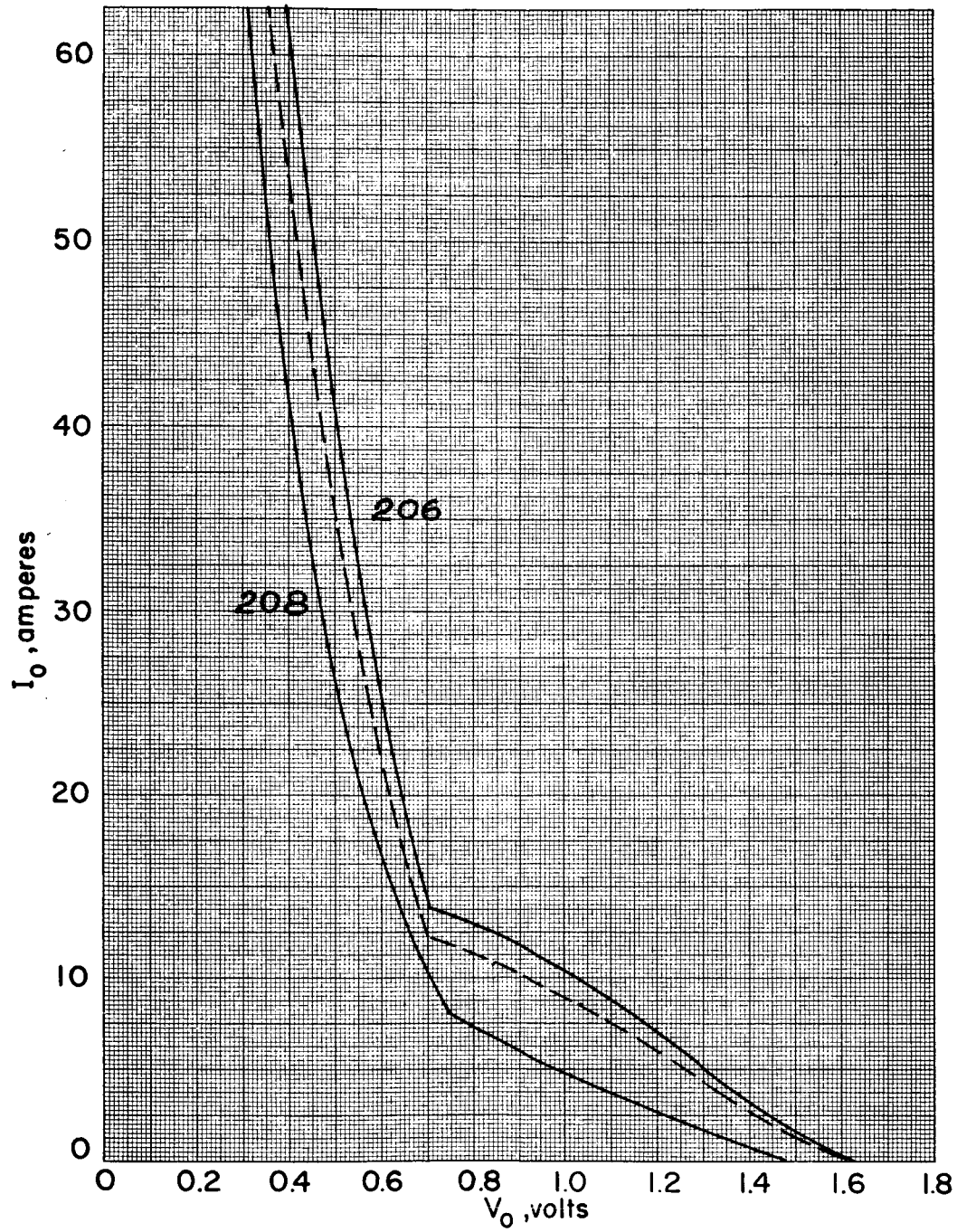


Figure 4

8270

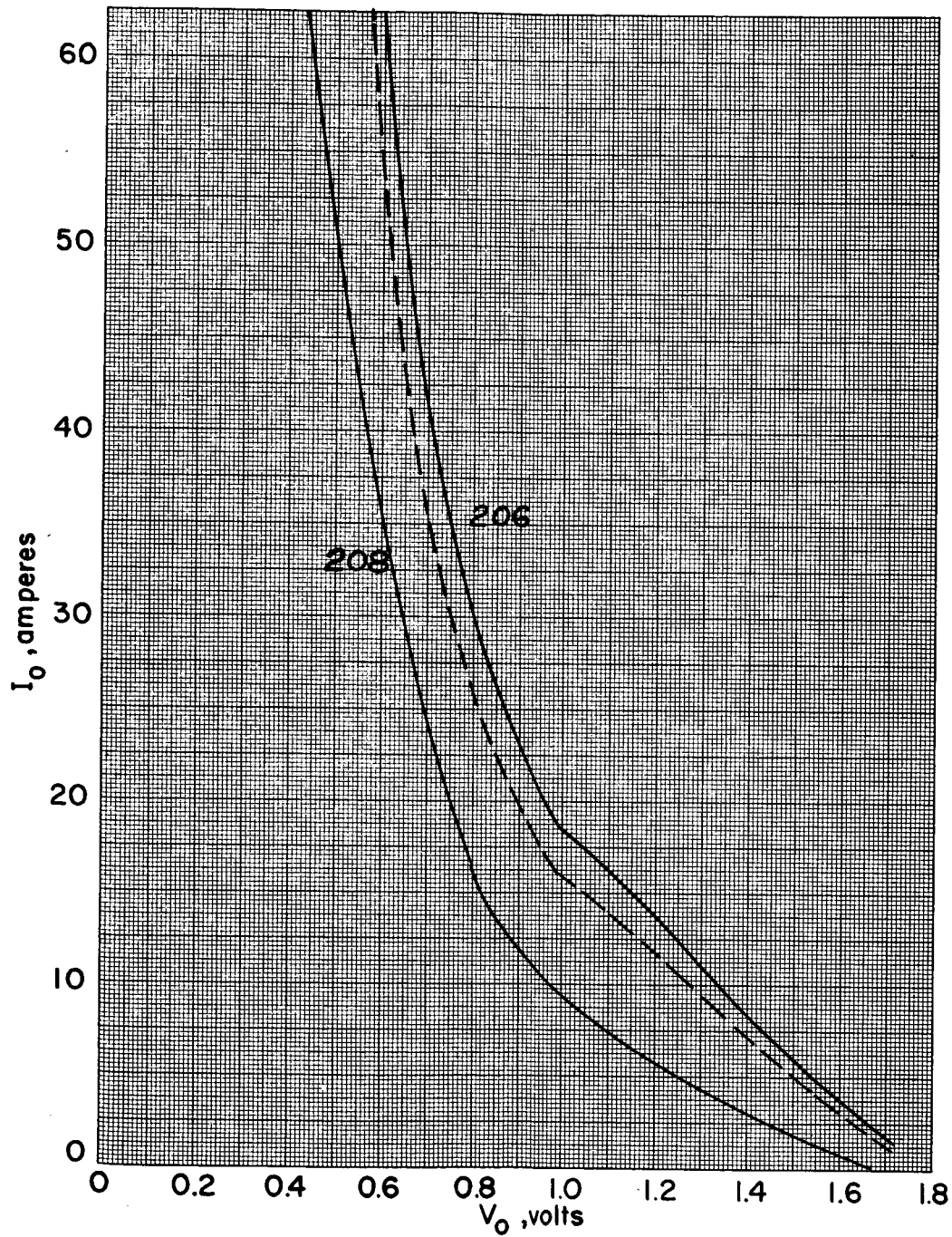


Figure 5

8271

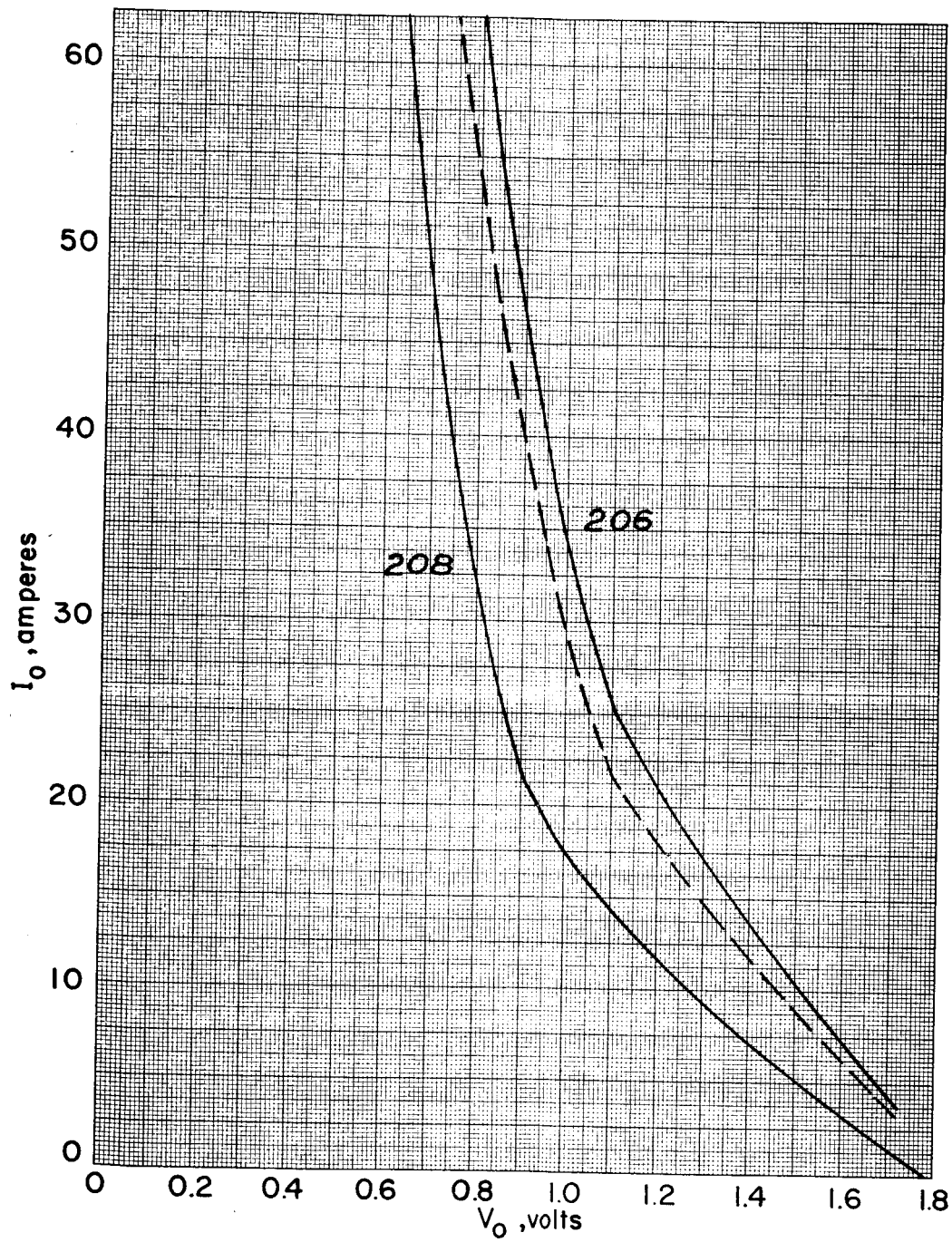


Figure 6



cesium pressure corresponding to a given output current increases with emitter temperature. This type of voltage shift is characteristic of a difference in interelectrode spacing, and because, in the extinguished mode, converter T-208 has a lower output than converter T-206, the indication is that converter T-206 has a larger spacing.

Such diagnosis is confirmed by comparison of the cesium conduction data, which is given for the same two converters in Figure 3. The interelectrode spacing determines the slope of the plotted characteristics according to the formula given in the Sixth Quarterly Report:

$$d = \{ [0.0001475A(T_E - T_C)(T_E + T_C)/(\partial Q/\partial p)]^{0.5} - 0.006(T_E + T_C) \} / p$$

where d is the spacing in mils, A is the interelectrode area in cm^2 , T_E and T_C are the emitter and collector temperatures in $^\circ\text{K}$, $\partial Q/\partial p$ is the slope of the characteristics given in Figure 3, and p is the pressure in torr.

Calculations for converters T-206 and T-208 at various pressures yield the following results:

	206		208	
p , torr	8	12	8	12
A , cm^2	2.52		2.16	
T_E , $^\circ\text{K}$	1990 $^\circ\text{K}$		2000 $^\circ\text{K}$	
T_C , $^\circ\text{K}$	861	875	880	885
$\partial Q/\partial p$, $\frac{\text{watts}}{\text{torr}}$	1.60	1.05	0.90	0.50
d , mils	1.29	1.38	2.06	2.33



and it can be seen that the spacing of converter T-206 has an average value of 1.33 mils, while that of converter T-208 has an average value of 2.20 mils. The actual magnitude of spacings ought to be somewhat larger because only the interelectrode area is assumed to contribute to heat conduction through the cesium, and in reality a larger area is involved. Nevertheless, the cesium conduction experiment does confirm that converter T-208 has an interelectrode spacing about 65% larger than that of converter T-206.

The above arguments tend to explain the performance differences between the two converters, and indicate that these can be eliminated by the use of more refined assembly techniques that would avoid an excessively large spacing, and also by utilizing a larger portion of the space available to develop collector area.

The lower performance of T-208 is not the only problem observed in this converter: Figure 2 shows that the dynamic data cannot be reproduced statically at high output currents. This is a typical indication of collector overheating. Figure 7 shows a comparison of the electron-bombardment power required to develop a given output current at output voltages of 0.8 and 1.0 volt for both converters T-206 and T-208. Again, it may be seen that at low currents (below 15 amperes) both converters are similar, but at higher input powers the additional input power in converter T-208 is used to overcome the high emitter temperatures that result from the inability to produce more output current. This is additional evidence of collector overheating. The collector overheating problem has now been traced to an excessive restriction in the vapor channel in the heat pipe, and is explained in the following section.

8272

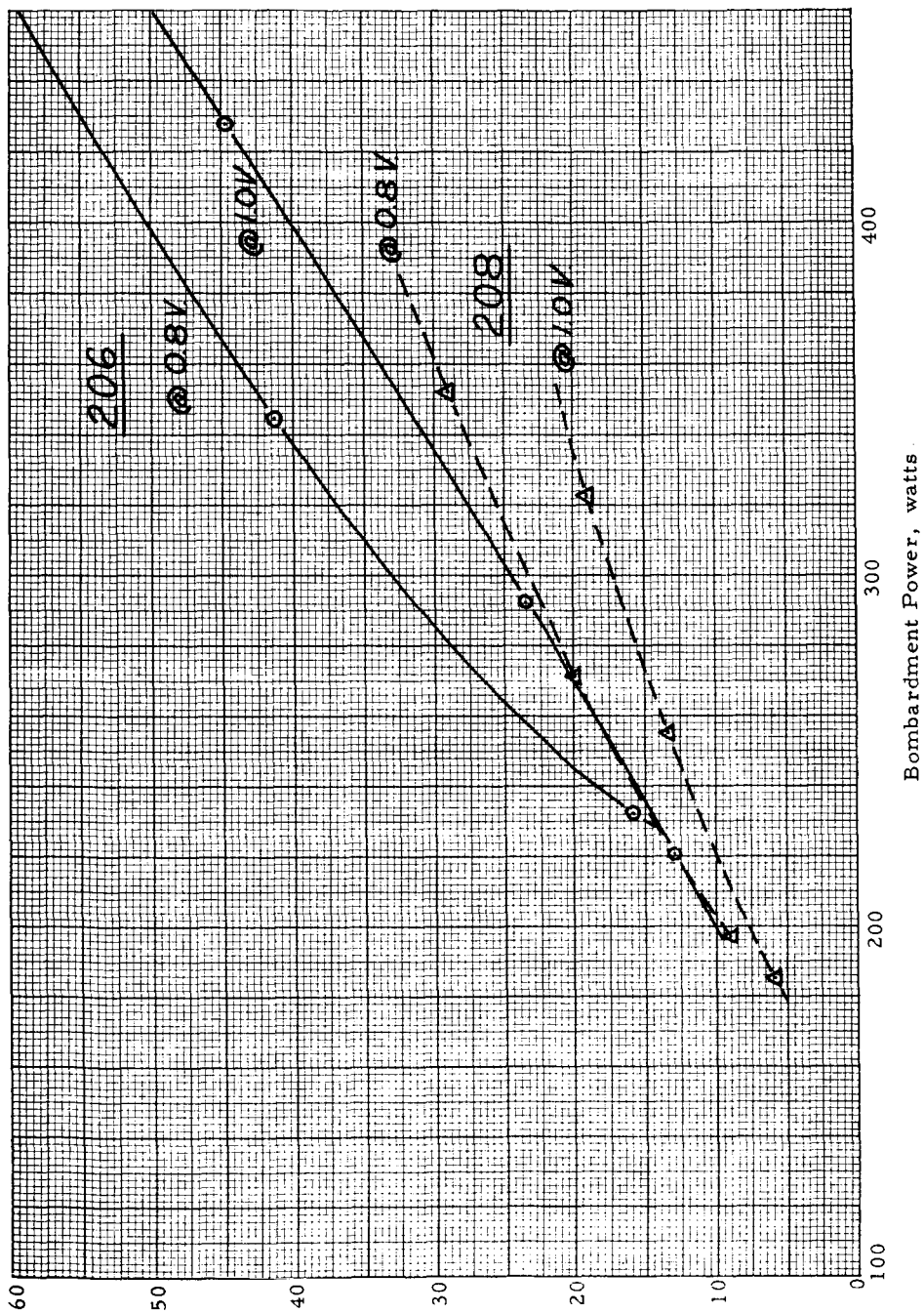


Figure 7



Heat Pipe Temperature Drop

The particular area of the heat pipe which is of interest in this discussion is the capillary structure at the heat-receiving end. In most heat pipes the heat input is distributed over a cylindrical surface of relatively unobstructed construction; as a result the heat transfer fluxes are sufficiently small to justify the assumption that liquid evaporation occurs with no significant temperature drop. In the present heat pipe design, the evaporating conditions are more severe, and as a result the temperature drop for evaporation has reached a value of about 80°C, which raises the collector temperature excessively.

A temperature drop occurs at the liquid-vapor interface because evaporation at a finite rate can occur only when the atom rate of evaporation of the liquid exceeds the atom arrival rate from the vapor. From kinetic theory, the corresponding heat flux in the one-dimensional case (evaporation from a plane surface) is given by:

$$g \text{ (watts/cm}^2\text{)} = 7.66 \times 10^{-4} \Delta H \left[\frac{p_1}{\sqrt{m T_1}} - \frac{p_2}{\sqrt{m T_2}} \right]$$

where ΔH is the heat of evaporation in cal/gm-mole

p_1, p_2 are the saturation pressures in dynes/cm²

T_1, T_2 are the corresponding temperatures in °K

m is the molecular weight in grams

This relationship is plotted in Figure 8, assuming $p_2 = 0$. The curve corresponds to the rate of evaporation when the surface is exposed to a vacuum. The dashed line represents the rate corresponding to



sonic vapor velocity, and as can be seen, the evaporation from the liquid can never be throttled by sonic velocity of the vapor phase.

In converter T-208, the heat transfer rate is given at an emitter temperature of 2000°K by the equation:

$$Q_{\text{collector}} = 105.7 + 1.92 I_o$$

At an output current of 83 amperes, the collector heat transfer would be 265.7 watts. The projected area of the heat pipe evaporator to handle this heat transfer is a circle approximately 0.590 in. in diameter, or 1.77 cm². The design heat transfer rate is then 265.7/1.77 = 150 watts/cm². Figure 8 shows that this rate, at a collector temperature (temperature of the liquid) of 700°C, would require a vapor temperature of 697°C, for then the heat transfer of 3500 W/cm² corresponding to liquid evaporation would exceed the rate of arrival of atoms from the vapor by the desired 150 W/cm². In that case, the temperature drop across the liquid-vapor interface would be negligible. However, not all of the projected area of the heat pipe evaporator is used to develop a liquid-vapor interface in converter T-208. To begin with, the capillary screen has an open area of only approximately 25%, so that the evaporation rate from the liquid occurs at a heat transfer rate of 150/0.25 = 600 W/sq cm; furthermore, the perforated plate, part No. 15, which is placed against the back of the screen as a support, also obstructs a large portion of the available liquid-vapor interface. The holes in the plate represent an open area of 0.413 cm², which is 23.4% of the projected area. The actual heat-transfer flux at which the sodium would evaporate in the T-208 converter heat pipe is then 600/0.234 = 2560 w/cm². Figure 8 shows that, at a vapor saturation

8273

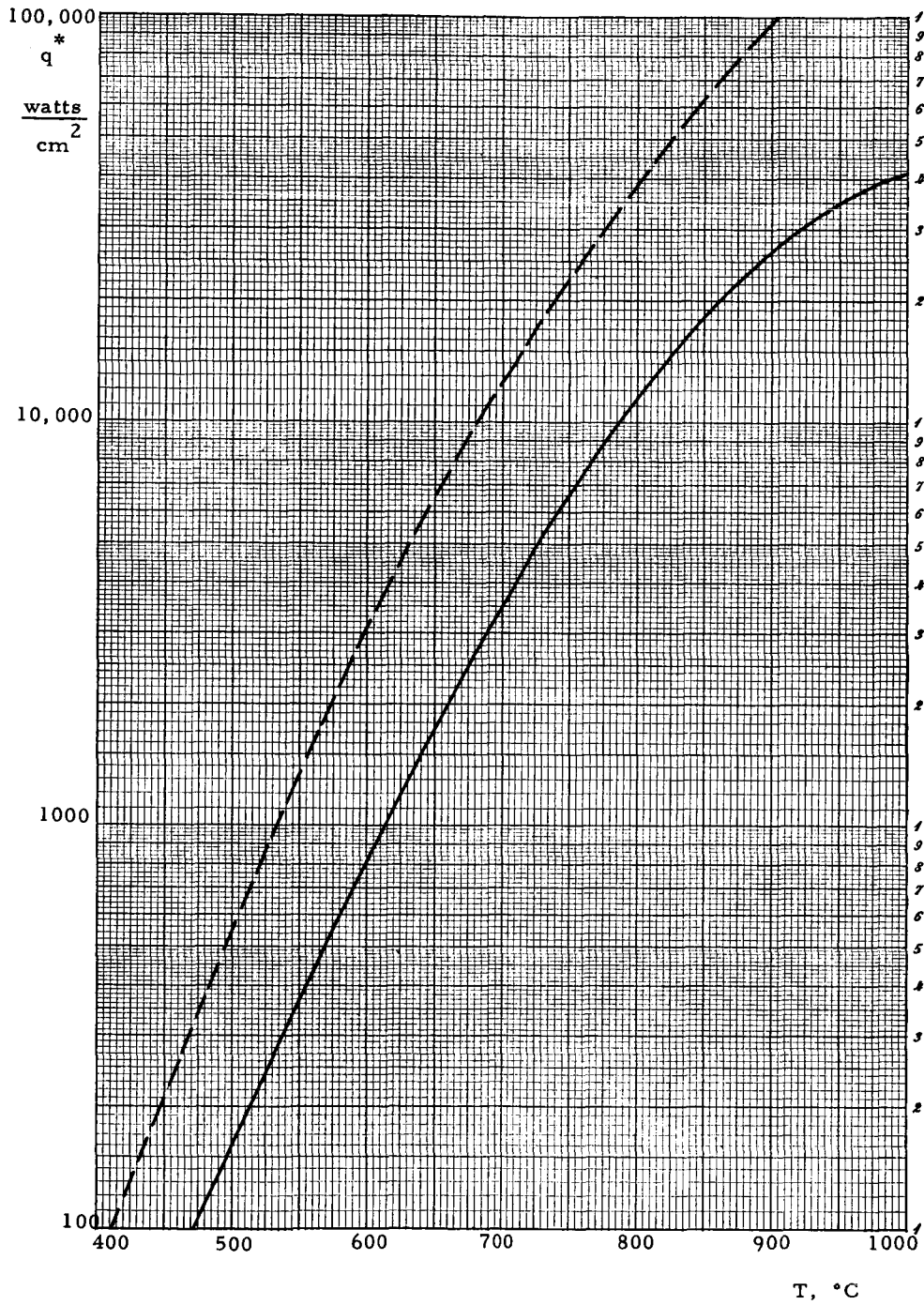


Figure 8



temperature of 700°C, the evaporating liquid would have to be at 785°C, or an increase of 85°C. If the holes in part No. 15 are replaced by a webbed support with 90% open area, the heat flux need only be $600/0.9 = 666 \text{ W/cm}^2$, and the liquid temperature corresponding to a 700°C vapor saturation temperature would then be 725°C, a reduction of 60°C in the collector temperature of T-208.

These temperature drops are difficult to detect in heat pipe models because they occur between the collector face and the heat pipe, and thermocouple instruments cannot be mounted readily on the heated face of the collector, which is exposed to electron bombardment during heating.

Plans for the Fabrication of Converter T-209

Pending JPL Approval Converter T-209 will be fabricated using a support plate at the heat pipe evaporator which will have a webbed construction to increase the open area. Also the length of the heat pipe radiator will be increased by 1 inch, which corresponds to a 36% increase in radiator area. Model T-209 would use an 0.200-in. - thick emitter to achieve a higher temperature uniformity over the emitter surface, a pressure-bonded collector without the cross-groove used in T-208, and a niobium-1% Zirconium 100-mesh screen capillary.

New Technology

No items of new technology have been included in this report.



THERMO ELECTRON

C O R P O R A T I O N

APPENDIX



Converter No. T-208

Run No. 1, 2 & 3

Observer P. Brosen

VARIABLE		1	2	3	4	5	6	7	8	9	10
Date	1968	2-26	2-26	2-26	2-26	2-26	2-26	2-26	2-26	2-26	2-26
Time		14:43	14:54	15:01	15:06	15:21	15:30	15:37	15:44	16:15	16:19
Elapsed Time, Hours		1.4	1.6	1.7	1.8	2.1	2.2	2.3	2.5	3.0	3.1
$T_0, ^\circ\text{C}$	(1)	1721	1725	1725	1725	1629	1629	1629	1629	1533	1533
T_0 Corrected, $^\circ\text{C}$		1726	1730	1730	1730	1631	1631	1631	1631	1532	1532
$\Delta T_{\text{Bell Jar}}, ^\circ\text{C}$		14	14	14	14	11	11	11	11	8	8
$T_H, ^\circ\text{C}$		1740	1744	1744	1744	1642	1642	1642	1642	1540	1540
$\Delta T_E, ^\circ\text{C}$	(2)	13	17	17	17	15	16	16	16	13	13
$T_E, ^\circ\text{K}$		2000	2000	2000	2000	1900	1900	1900	1900	1800	1800
V_0 , volts		—	—	—	—	—	—	—	—	—	—
I_0 , amps		18	28	28	28	20	24	24	24	12	20
P_0 , watts		—	—	—	—	—	—	—	—	—	—
I-V Trace No.		1	2	3	4	5	6	7	8	9	10
T_R	mv	12.4	13.4	14.3	15.2	12.5	13.4	14.3	15.2	12.7	13.4
	$^\circ\text{C}$	304	329	350	372	307	329	350	372	312	329
	$^\circ\text{K}$	577	602	623	645	580	602	623	645	585	602
T_C	mv	26.4	28.1	28.7	28.3	25.8	26.8	26.9	26.9	24.8	25.2
	$^\circ\text{C}$	635	675	690	680	621	644	647	647	597	607
	$^\circ\text{K}$	908	948	963	953	894	917	920	920	870	880
T_C base inner	mv	—	—	—	—	—	—	—	—	—	—
	$^\circ\text{C}$										
T_C base outer	mv	—	—	—	—	—	—	—	—	—	—
	$^\circ\text{C}$										
T_{Radiator}	mv	—	—	—	—	—	—	—	—	—	—
	$^\circ\text{C}$										
V_{eb} , volts		975	971	969	969	978	976	975	975	981	981
I_{eb} , mA		243.0	280.7	301.7	300.0	221.2	238.8	248	248	198.4	203.3
E_{Filament} , volts		4.8	5.0	5.0	5.0	4.8	4.9	4.9	4.9	4.8	4.8
I_{Filament} , amps		19	19	19.5	19.5	19.0	19.0	19.0	19.0	19.0	19.5
$I_{\text{Coll. Heater}}$, amps		—	—	—	—	—	—	—	—	—	—
$I_{\text{Res. Heater}}$, amps		0	.45	1.50	1.80	0	1.45	1.58	2.18	1.30	1.63
Vacuum, 10^{-6} mm Hg		18	18	18	18	16	14	14	14	12	12
Measured Efficiency, % P_{eb}		236.9	272.8	292.3	290.7	216.3	232.8	241.8	241.8	194.6	199.4

NOTES: (1) PYROMETER CORRECTIONS: -1°C @ 1500°C ; $+2^\circ\text{C}$ @ 1600°C ; $+5^\circ\text{C}$ @ 1700°C
BELL JAR CORRECTIONS: $+8^\circ\text{C}$ @ 1500°C ; $+11^\circ\text{C}$ @ 1600°C ; $+14^\circ\text{C}$ @ 1700°C

(2) $\Delta T_E = 10 + 0.25 I$

(3) HIGHER T_R OBSERVED (THICK WALLED CS TUBE).



Converter No. T-208

Run No. 3 1/4

Observer P. Brosnan

VARIABLE		1	2	3	4	5	6	7	8	9	10
Date		2-26	2-26	2-26	—	—	—	—	—	—	2-26
Time		16:27	16:30	17:00	—	—	—	—	—	—	17:23
Elapsed Time, Hours		3.2	3.3	3.7	—	—	—	—	—	—	4.0
T ₀ , °C		1535	1535	1718	—	—	—	—	—	—	1718
T ₀ Corrected, °C		1534	1534	1723	—	—	—	—	—	—	1723
ΔT _{Bell Jar} , °C		8	8	14	—	—	—	—	—	—	14
T _H , °C		1542	1542	1737	—	—	—	—	—	—	1737
ΔT _E , °C		15	15	10	—	—	—	—	—	—	10
T _E , °K		1800	1800	2000	—	—	—	—	—	—	2000
V ₀ , volts		—	—	—	—	—	—	—	—	—	—
I ₀ , amps		20	20	0	0	0	0	0	0	0	0
P ₀ , watts		—	—	—	—	—	—	—	—	—	—
I-V Trace No.		11	12	—	—	—	—	—	—	—	—
T _R	mv	14.3	15.2	11.7	12.5	13.0	14.0	14.5	15.0	16.0	17.0
	°C	350	372	288	307	319	343	355	367	391	414
	°K	623	645	561	580	592	616	628	640	664	687
T _C	mv	25.6	25.7	24.2	24.4	24.6	24.9	25.0	25.2	25.4	25.6
	°C	616	618	583	588	593	600	602	607	612	616
	°K	889	891	856	861	866	873	875	880	885	889
T _C base inner	mv	—	—	—	—	—	—	—	—	—	—
	°C	—	—	—	—	—	—	—	—	—	—
T _C base outer	mv	—	—	—	—	—	—	—	—	—	—
	°C	—	—	—	—	—	—	—	—	—	—
T _{Radiator}	mv	—	—	—	—	—	—	—	—	—	—
	°C	—	—	—	—	—	—	—	—	—	—
V _{eb} , volts		980	980	983.2	982.7	982.9	982.2	981.7	981.5	981.1	*
I _{eb} , mA		207.3	206.9	221.1	225.5	227.6	232.0	233.8	236.4	238.6	*
E _{Filament} , volts		4.8	4.8	4.8	—	—	—	—	—	—	4.8
I _{Filament} , amps		19.0	19.0	19.0	—	—	—	—	—	—	19.0
I _{Coll. Heater} , amps		—	—	—	—	—	—	—	—	—	—
I _{Res. Heater} , amps		2.30	2.58	0	1.12	1.54	2.01	2.16	2.45	2.89	3.20
Vacuum, 10 ⁻⁶ mm Hg		12	12	12	—	—	—	—	—	—	12
Measured Efficiency, %		203.1	202.7	217.4	221.7	223.7	228.0	229.5	232.0	234.1	—

NOTES: * NO READING BECAUSE SERVO-OPTICS WERE ACCIDENTALLY DISPLACED.



Converter No. T-208

Run No. 5 & 6

Observer P. Brosius & E. Peredetto

VARIABLE		1	2	3	4	5	6	7	8	9	10
Date		2-26	2-27	2-27	2-27	2-27	2-27	2-27	2-27	2-27	2-27
Time		17:36	11:24	11:32	11:44	11:57	13:10	13:25	13:36	13:46	13:55
Elapsed Time, Hours		4.3	22.1	22.3	22.5	22.7	23.9	24.2	24.4	24.5	24.7
T_0 , °C		1681	1681	1681	1681	1681	1587	1587	1587	1587	1587
T_0 Corrected, °C		1686	1686	1686	1686	1686	1589	1589	1589	1589	1589
$\Delta T_{\text{Bell Jar}}$, °C		14	14	14	14	14	11	11	11	11	11
T_H , °C		1700	1700	1700	1700	1700	1600	1600	1600	1600	1600
ΔT_E , °C		11	12	13	15	18	10	11	11	12	13
T_E , °K		1962	1961	1960	1958	1955	1863	1862	1862	1861	1860
V_0 , volts		1.400	1.200	1.000	.800	.600	1.400	1.200	1.000	.800	.600
I_0 , amps		5.1	9.0	13.4	20.1	32.2	2.0	3.1	5.8	9.0	14.3
P_0 , watts		7.14	10.8	13.4	16.1	19.3	2.8	3.7	5.8	7.2	8.6
I-V Trace No.		—	—	—	—	—	—	—	—	—	—
T_R	mv	14.2	13.3	13.5	13.9	14.3	11.5	11.9	12.1	12.5	13.0
	°C	348	326	331	341	350	283	292	297	307	319
	°K	621	599	604	614	623	556	565	570	580	592
T_C	mv	24.8	25.3	26.0	27.0	28.7	22.7	16.6	17.0	24.0	24.9
	°C	597	609	626	649	690	548	(1)	(1)	579	600
	°K	870	882	899	922	963	821	—	—	852	873
T_C base inner	mv	—	—	—	—	—	—	—	—	—	—
	°C										
T_C base outer	mv	—	—	—	—	—	—	—	—	—	—
	°C										
T_{Radiator}	mv	—	—	—	—	—	—	—	—	—	—
	°C										
V_{eb} , volts		981	975	973	970	965	984	984	982	980	977
I_{eb} , mA		219.8	246.5	262.7	279.9	315.8	181.2	183.4	188.9	201.1	218.1
E_{Filament} , volts		4.8	4.8	4.8	5.0	5.0	4.8	4.8	4.8	4.8	4.9
I_{Filament} , amps		19.0	19.0	19.0	19.0	19.0	18.0	18.4	18.5	18.6	18.8
$I_{\text{Coll. Heater}}$, amps		—	—	—	—	—	—	—	—	—	—
$I_{\text{Res. Heater}}$, amps		2.07	1.43	1.35	1.41	1.45	0	1.0	1.26	1.25	1.85
Vacuum, 10^{-6} mm Hg		12	10	10	10	10	10	10	10	10	10
Measured Efficiency, % P_{eb}		215.6	240.3	255.6	271.5	304.7	178.3	180.5	185.5	197.1	213.1

NOTES: (1) INCORRECT READING, T_C SHORTED TO POTENTIOMETER WITH SETTING FOR T_R



Converter No. T-208

Run No. 7

Observer E. Peredetto & P. Brosens

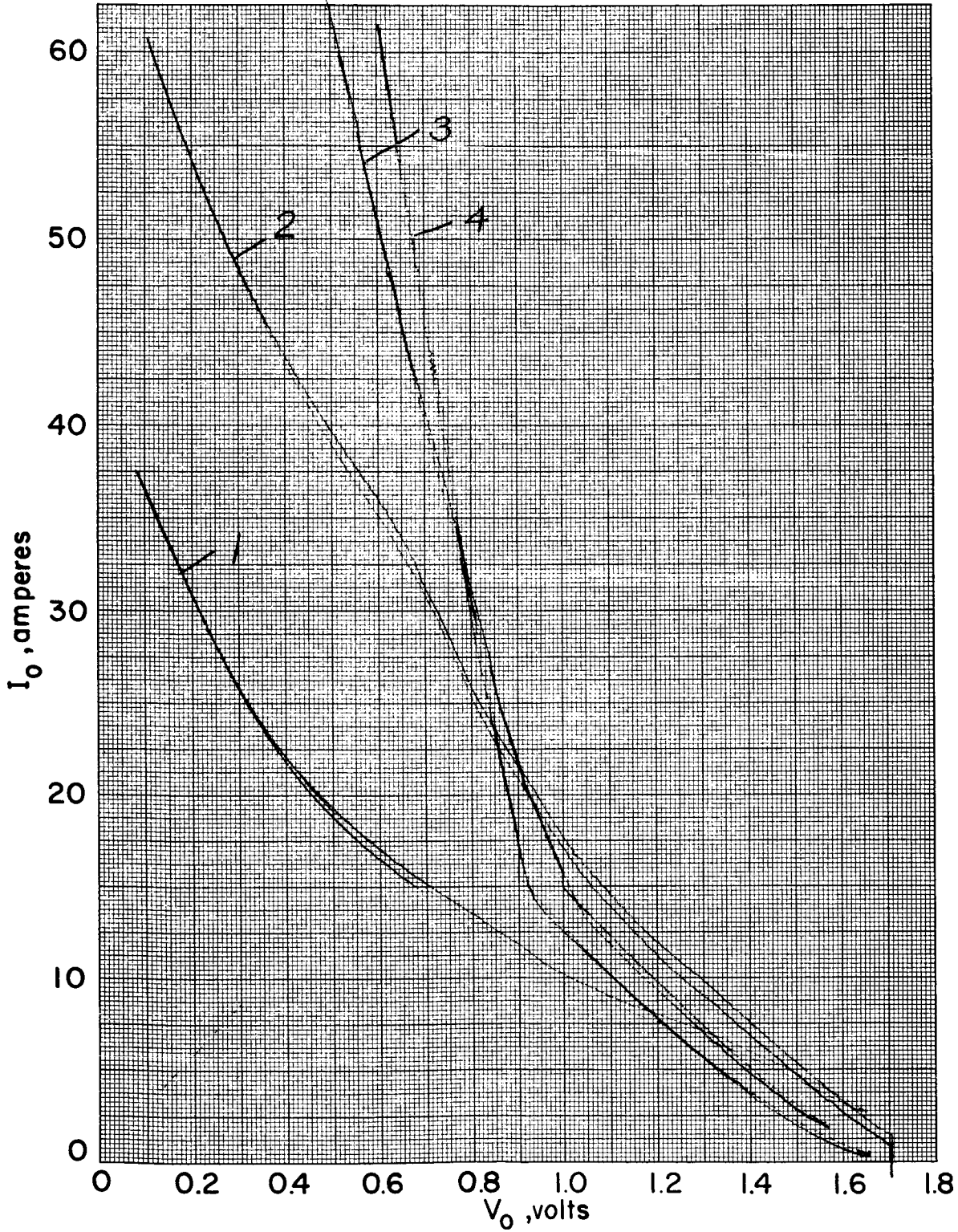
VARIABLE		1	2	3	4	5	6	7	8	9	10
Date		2-27	2-27	2-27	2-27	2-27					
Time		14:43	14:50	14:56	15:03	15:16					
Elapsed Time, Hours		25.4	25.5	25.6	25.8	26.0					
T_0 , °C		1775	1775	1775	1775	1775					
T_0 Corrected, °C		1783	1783	1783	1783	1783					
$\Delta T_{\text{Bell Jar}}$, °C		17	17	17	17	17					
T_H , °C		1800	1800	1800	1800	1800					
ΔT_E , °C		12	13	15	17	20					
T_E , °K		2061	2060	2058	2056	2053					
V_0 , volts		1.400	1.200	1.000	.800	.600					
I_0 , amps		7.4	12.4	19.0	28.9	41.4					
P_0 , watts		10.4	14.9	19.0	23.1	24.8					
I-V Trace No.		—	—	—	—	—					
T_R	mv	13.7	13.9	14.0	14.7	15.0					
	°C	336	341	343	360	367					
	°K	609	614	616	633	640					
T_C	mv	26.6	27.2	28.1	29.3	31.0					
	°C	640	654	675	704	744					
	°K	913	927	948	977	1017					
T_C base inner	mv	—	—	—	—	—					
	°C										
T_C base outer	mv	—	—	—	—	—					
	°C										
T_{Radiator}	mv	—	—	—	—	—					
	°C					*					
V_{eb} , volts		972	969	966	962	957					
I_{eb} , mA		295.5	310.8	333.9	366.4	408.3					
E_{Filament} , volts		4.9	5.0	5.0	5.0	5.1					
I_{Filament} , amps		19.0	19.0	19.0	19.0	19.2					
$I_{\text{Coll. Heater}}$, amps		—	—	—	—	—					
$I_{\text{Res. Heater}}$, amps		1.48	1.36	1.42	1.38	1.40					
Vacuum, 10^{-6} mm Hg		10	10	10	10	10					
Measured Efficiency, %		287.2	301.2	322.5	352.5	390.7					

NOTES: * END OF TEST



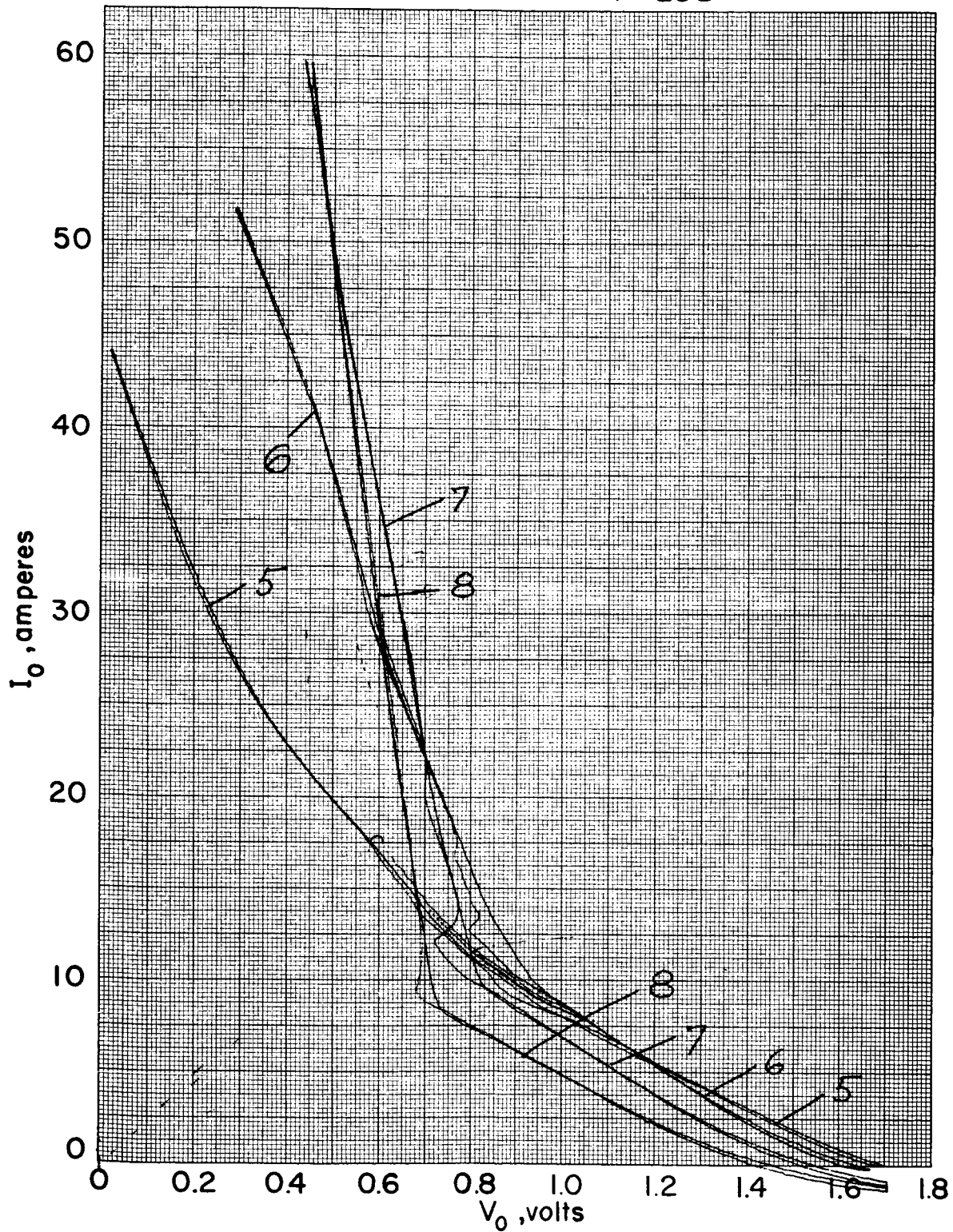
8274

T-208 1 → 4



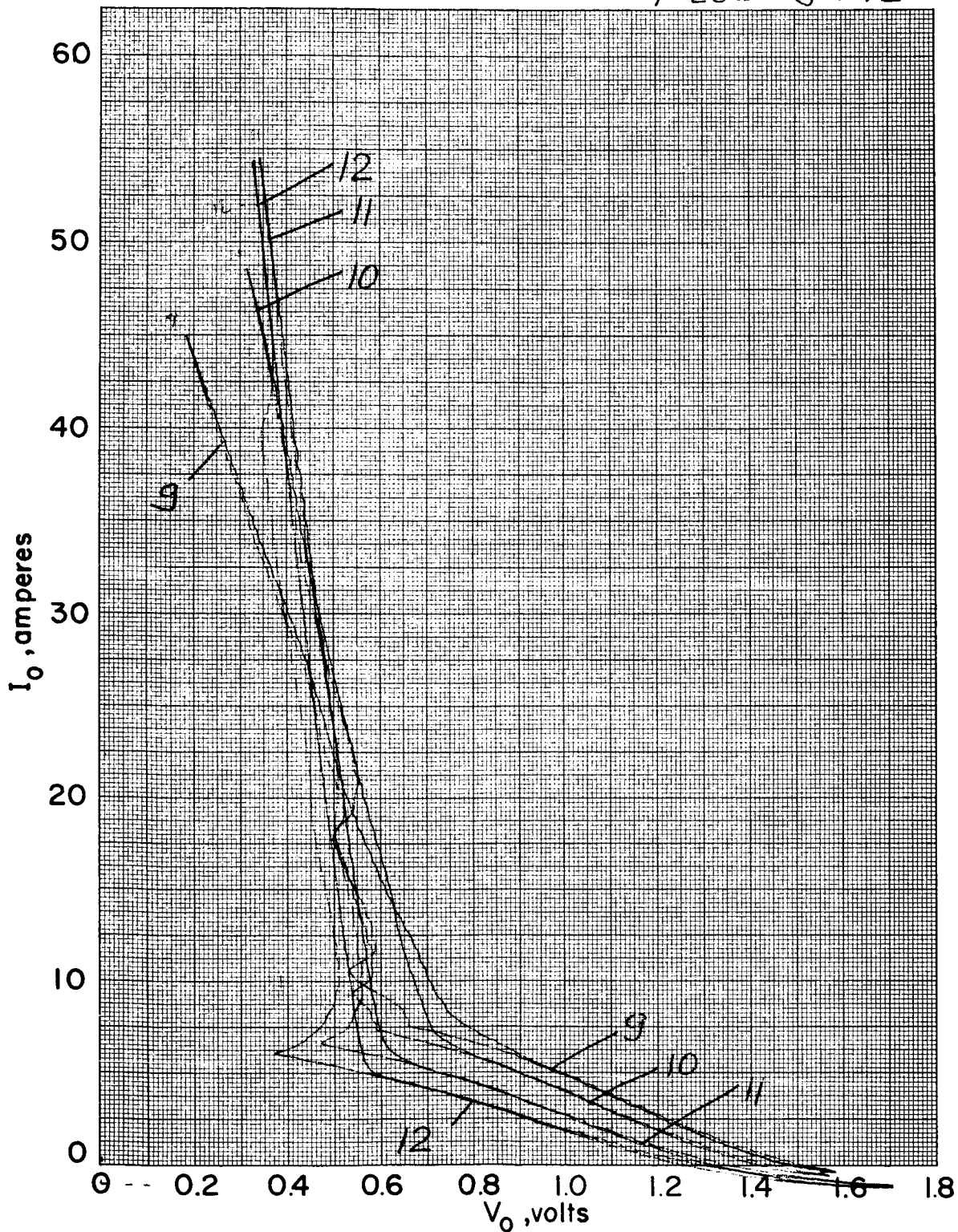
8275

T-208 5 → 8



8276

T-208 9 → 12



8277

PYROMETER AND BELL JAR CALIBRATION RECORD

 Sheet 1 of 2

 Instrument No. M-5217

 Date 2-23-68

 NBS Lamp No. 186792

 Temp. Level, °C 1600

		OBSERVER 1	OBSERVER 2
		Name <u>P. Brosnan</u>	Name <u>E. Paredello</u>
	Lamp Current, Amps.	9.69	9.69
	Lamp Brightness Temp., °C	1600°C	1600°C
PYROMETER CALIBRATION	Bright to Dark Reading, °C	1602	1596
	Dark to Bright Reading, °C	1598	1594
	Dark to Bright Reading, °C	1599	1600
	Bright to Dark Reading, °C	1600	1597
	Average Reading, °C	1599.75	1596.75
	Correction to be Applied to Pyrometer, °C	+ 0.25	+ 3.25
BELL JAR CALIBRATION	Bright to Dark Reading, °C	1588	1587
	Dark to Bright Reading, °C	1582	1587
	Dark to Bright Reading, °C	1585	1587
	Bright to Dark Reading, °C	1583	1585
	Average Reading, °C	1584.50	1586.50
	Bell Jar Correction, °C (<i>incl pyro</i>)	+ 15.25	+ 10.25

 Average of Pyrometer Corrections, Observers 1 & 2, °C + 1.75

 Average of Bell Jar Corrections, Observers 1 & 2, °C + 11.0°C

8278

PYROMETER AND BELL JAR CALIBRATION RECORD

 Sheet 2 of 2

 Instrument No. M-5217

 Date 2-23-68

 NBS Lamp No. 186792

 Temp. Level, °C 1700

		OBSERVER 1	OBSERVER 2
		Name <u>P. Brosnan</u>	Name <u>E. Peradillo</u>
	Lamp Current, Amps.	10.58	10.58
	Lamp Brightness Temp., °C	1700.0	1700.0
PYROMETER CALIBRATION	Bright to Dark Reading, °C	1695	1695
	Dark to Bright Reading, °C	1696	1693
	Dark to Bright Reading, °C	1696	1693
	Bright to Dark Reading, °C	1696	1693
	Average Reading, °C	1695.75	1693.50
	Correction to be Applied to Pyrometer, °C	+ 4.25	+ 6.50
BELL JAR CALIBRATION	Bright to Dark Reading, °C	1681	1682
	Dark to Bright Reading, °C	1678	1679
	Dark to Bright Reading, °C	1682	1683
	Bright to Dark Reading, °C	1680	1681
	Average Reading, °C	1680.25	1681.25
	Bell Jar Correction, °C (incl. pyro)	+ 19.75	+ 18.75

 Average of Pyrometer Corrections, Observers 1 & 2, °C + 5.35

 Average of Bell Jar Corrections, Observers 1 & 2, °C + 14.25